J Fluoresc (2009) 19:291–302
DOI 10.1007/s10895-008-0415-1

ORIGINAL PAPER

Study of Protein–Probe Interaction and Protective Action of Surfactant Sodium Dodecyl Sulphate in Urea-Denatured HSA using Charge Transfer Fluorescence Probe Methyl Ester of *N*,*N*-Dimethylamino Naphthyl Acrylic Acid

Subrata Mahanta · Rupashree Balia Singh · Nikhil Guchhait

Received: 20 May 2008 / Accepted: 20 August 2008 / Published online: 12 September 2008

Abstract We have demonstrated that the intramolecular charge transfer (ICT) probe Methyl ester of *N*,*N*-dimethylamino naphthyl acrylic acid (MDMANA) serves as an efficient reporter of the proteinous microenvironment of Human Serum Albumin (HSA). This work reports the binding phenomenon of MDMANA with HSA and spectral modulation thereupon. The extent of binding and free energy change for complexation reaction along with efficient fluorescence resonance energy transfer from Trp-214 of HSA to MDMANA indicates strong binding between probe and protein. Fluorescence anisotropy, red edge excitation shift, acrylamide quenching and time resolved measurements corroborate the binding nature of the probe with protein and predicts that the probe molecule is located at the hydrophobic site of the protein HSA. Due to the strong binding ability of MDMANA with HSA, it is successfully utilized for the study of stabilizing action of anionic surfactant Sodium Dodecyl Sulphate to the unfolding and folding of protein with denaturant urea in concentration range 1M to 9M.

Keywords Methyl ester of *N*,*N*-dimethylamino naphthyl acrylic acid · Human serum albumin · Sodium dodecyl sulphate · Fluorescence · Protein

S. Mahanta · R. B. Singh · N. Guchhait (✉)
Department of Chemistry, University of Calcutta,
92 A. P. C. Road,
Kolkata 700009, India
e-mail: nguchhait@yahoo.com

Introduction

Human Serum Albumin (HSA) is the most abundantly found in blood plasma and is often considered as transport protein. The molecule HSA is circulated in the body and acts as carriers for numerous exogenous and endogenous compounds [1]. It is a large protein formed from a single polypeptide chain of 585 residues [1–5]. The structure of HSA is divided into three major domains and contains a total of 17 disulphide bonds. Despite the size and structural complexity of HSA, it contains a single Tryptophan (Trp) at position 214 in the domain II [2, 5] and one free cysteine residue at the position 34 in domain I. In general, albumins are characterized by low tryptophan and high cysteine contents. The presence of free thiol allows site-specific labeling of the protein with chromophore or fluorescence probes. The protein HSA has the ability to bind several ligands, including small aromatic and heterocyclic carboxylic acids such as nonsteroidal antiflammatory drugs [6]. Two main approaches have been adopted in the ligand–protein binding studies. Some groups have studied the *in vivo* consequences of binding of drugs and other metabolites to serum albumins. The others have examined the binding mechanism using absorption, fluorescence, circular dichroism spectroscopy. Based on such studies, information on the binding process of many exogenous ligands like long chain fatty acids, amino acids, metals, drugs, bilirubin etc have been reported at the molecular level [6–10]. It has also been considered that such binding can increase the solubility of ligands and there are reports that the toxicity of some ligands like bilirubin decreased on binding to albumins.

The native structure of globular protein such as HSA and the folding and unfolding processes of protein are important research for long time. It is well known that urea is a strong denaturant for the native structure of globular protein HSA. Marcus and Krush studied the effect of surfactants on the urea denaturation of HSA by means of optical rotary dispersion spectroscopy [11]. Recently, Moriyama et al. studied the effect of Sodium Dodecyl Sulphate (SDS) on the helicities of urea denatured HSA by means of circular dichroism spectroscopy [12]. They studied the structural changes of HSA in the urea solution in 0.10M phosphate buffer solution of pH 7.0. It is reported that the helicity of HSA does not decrease remarkably before 3M urea solution and it decreases up to 13% at 9M urea solution. Considering SDS as denaturing agent, Marcus et al. found that the helicity of HSA decrease from 66% to 47% in the SDS solution [11]. The observed helicity changes of urea-denatured HSA upon the addition of SDS are roughly divided into three ranges: (i) A range below 3M where the helicity only decreases, (ii) a range between 4M to 8M where the helicity initially increases then sharply deceases, (iii) a range probably above 9M where the helicity only increases with increasing SDS concentration. It is reported that the decreasing of helicity of HSA with SDS in absence or presence of urea (below 3M) is more or less similar [12].

Fluorescence spectroscopy serves as an important tool for monitoring the organization and dynamics of biological and model membranes due to suitable time-scale, high sensitivity and lack to external perturbation. Fluorescence probe technique is one of the cheapest and least cumbersome methods used for studying the polarity of protein cavities [7, 13–19]. Use of extrinsic probes for elucidation of protein structure and dynamics using both steady state and time-resolved fluorescence techniques has attracted lot of attention compared to the use of intrinsic probe [20–22]. A number of studies show that some synthetic and therapeutically active naturally occurring flavonols can serve as excellent monitors of the microenvironments of biologically relevant systems [13]. Charge transfer (CT) fluorescent probes such as Prodan [7] and Nile Red [15] that exhibit both changes in fluorescence intensity and spectral shift have been successively used for protein binding studies and displacement studies and analysis of protein–probe complexation equilibria. Extrinsic probes are more successfully applied for studying conformational changes of the protein structure with variation of its solvent characteristics etc. instead of direct monitoring of the tryptophanyl fluorescence [17, 13–21].

In the present work, intramolecular charge transfer (ICT) probe MDMANA [23] is used to study the modulation of photophysics upon binding with HSA. The advantages of using MDAMANA as fluorescence probe are i) it is neutral and hydrophobic in nature and ii) it has solvent dependent CT emission band. Hydrophobic nature of the probe molecule makes it possible to remain solubilized in the protein microenvironment. In spite of the presence of CT species in the excited state, lack of any residual charge on the molecule makes it an efficient fluorescent probe. MDMANA binds strongly to HSA and this is well reflected in the values of binding constant (K) and free energy change (ΔG). The penetration of MDMANA into the hydrophobic cavity of HSA is evident from the FRET. Turro et al. [24] and Das et al. [25] have studied the destabilizing action of SDS on the Bovine Serum Albumin (BSA). We have utilized self designed and synthetic probe for studying the protective action of SDS binding on the urea-denatured HSA. Very low concentration of SDS helps to restore the native conformation of HSA to a great extent in the presence of strong denaturant urea. The sensitivity of the CT band to change in polarity of the microenvironment helps to study the protective action of SDS on urea denatured HSA.

Experimental section

MDMANA (Scheme I) was synthesized using literature procedure [23]. Tris buffer purchased from SRL, India was used for the preparation of Tris–HCl buffer (0.01M) of pH=7. Human Serum Albumin (HSA) from Sigma and Sodium Dodecyl Sulphate and Urea purchased from SRL, India were used as supplied. Triple distilled water was used for the preparation of solutions. The purity of all solvents in the wavelength range used for fluorescence measurement was checked before preparation of solutions.

The absorption and emission measurements were done by Hitachi UV–Vis U-3501 spectrophotometer and Perkin Elmer LS-50B spectrophotometer, respectively. In all measurements, the sample concentration was maintained within the range of 10^{-6} mol/dm^3 in order to avoid aggregation and reabsorption effects.

Fluorescence quantum yield (Φ_f) was determined using β-naphthol as the secondary standard (Φ_f=0.23 in methyl-cyclohexane) using the following equation [26]:

$$\frac{\Phi_S}{\Phi_R} = \frac{A_S}{A_R} \times \frac{(Abs)_R}{(Abs)_S} \times \frac{n_S^2}{n_R^2} \quad (1)$$

Scheme I Structure of MDMANA

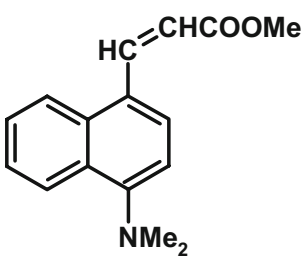

Where Φ_S and Φ_R are the quantum yields, A_S and A_R are the integrated fluorescence area, and $(Abs)_S$ and $(Abs)_R$ are absorbances for the sample and reference, respectively. n_S and n_R are the refractive index for the sample and reference solution, respectively.

The measurements of steady state anisotropy were carried out using the same Perkin Elmer LS-50B spectrophotometer. The steady state anisotropy r is defined as

$$r = (I_{VV} - G.I_{VH})/(I_{VV} + G.I_{VH}) \quad (2)$$

$$G = I_{HV}/I_{HH} \quad (3)$$

Where I_{VV} and I_{VH} are the emission intensities when the excitation polarizer is vertically oriented and the emission polarizer is oriented vertically and horizontally, respectively. G is the correction factor. The terms I_{VH} *and* I_{HH} are the emission intensity when the excitation polarization is horizontally oriented and the emission polarization is oriented vertically and horizontally respectively [27].

The experimental setup for picosecond TCSPC includes a picosecond diode laser at 408 nm (IBH, UK, NanoLED-07, s/n 0.3931) as light source [28]. The fluorescence signal was detected in magic angle (54.7° polarization using Hamamatsu MCP PMT (3809U). The typical system response of the laser system was 90 ps. The decays were analyzed using IBH DAS-6 decay analysis software. The fluorescence decay curves were analyzed by biexponential and triexponential fitting program of IBH. The average lifetimes were calculated using the equation [27]:

$$\langle \tau \rangle = \frac{\sum_i a_i \tau_i^2}{\sum_i a_i \tau_i} \quad (4)$$

Where τ_i and a_i are the fluorescence lifetime and its coefficient of the *i*th component, respectively.

Results and discussion

Spectroscopic properties of MDMANA and ICT reaction

The molecule MDMANA shows absorption maxima at ~350 nm for the $\pi\pi^*$ transition of the aromatic ring chromophore. Excitation of MDMANA at ~354 nm in water gives rise to dual fluorescence bands—a higher energy band at ~425 nm and a lower energy but relatively intense emission band at ~521 nm. This large Stokes-shifted emission band at 521 nm ($\Delta\nu$=9055 cm^{-1}) has been assigned to emission from the CT state of MDMANA based on the steady state absorption and emission study [23]. The CT emission band is observed in polar solvents whereas only the higher energy local emission (LE) band is observed in non-polar solvents [23]. As the CT band is sensitive to the nature of the solvents it gradually shifts to higher wavelength with increasing polarity and hydrogen bonding ability of the solvents (λ_{em}=493 nm in acetonitrile and λ_{em}=521 nm in water). Theoretical calculations using Density Functional Theory (DFT) predicts well photoinduced intramolecular charge transfer reaction by considering twisted intramolecular charge transfer (TICT) model. For the molecule MDMANA, the $-NMe_2$ group is already out of plane of the benzene ring and the N-atom of the $-NMe_2$ group is pyramidal in its global minimum state. Rotation of the donor group generates a stable twisted geometry in the excited state surface which leads to produce a solvents stabilized charge transfer state. The results of detailed calculation are described elsewhere [23].

Study of probe–protein complexation reaction

As seen in Fig. 1a (Inset), gradual addition of HSA to a solution of MDMANA in aqueous buffer (Tris buffer, 0.01M, pH=7.03) results in increase in absorbance with gradual shift of the absorption maxima to the red side (from~355 nm to ~363 nm). On the other hand, the position of the emission maxima (Fig. 1a & b) shows a blue shift (from ~521 nm in aqueous buffer to ~482 nm in presence of 100 μM of HSA) with manifold enhancement of emission intensity with addition of HSA. In fact the neutral and hydrophobic nature of the probe molecule favours better solubilization in the hydrophobic cavities of HSA. The decrease in polarity of the surrounding microenvironment of the probe inside the protein is reflected by the blue shift of the emission maxima of the probe. Usually, water acts as a quencher of CT emission and as the probe molecules are less exposed to water inside the hydrophobic cavity of HSA the possibility of non-radiative decay reduces to a great extent. Inside the protein cavity the polarity is less compare to the outer side, resulting in an increase in energy gap between the CT state and the triplet/ground states. According to the energy gap law this would lead to a reduction in the non-radiative decay and, hence, CT emission is enhanced in presence of protein. Increased quantum yield values with increasing concentration of HSA are also indicative of the same conclusion [13–17].

A quantitative estimate of binding of MDMANA to the hydrophobic cavity of HSA is determined using the Benesi–Hildebrand relation [29]. The complexation equilibrium can be described as follows

$$\text{MDMANA} + \text{HSA} \overset{K}{\leftrightarrow} \text{MDMANA : HSA} \quad (5)$$

$$K = \frac{[\text{MDMANA : HSA}]}{[\text{MDMANA}][\text{HSA}]} \quad (6)$$

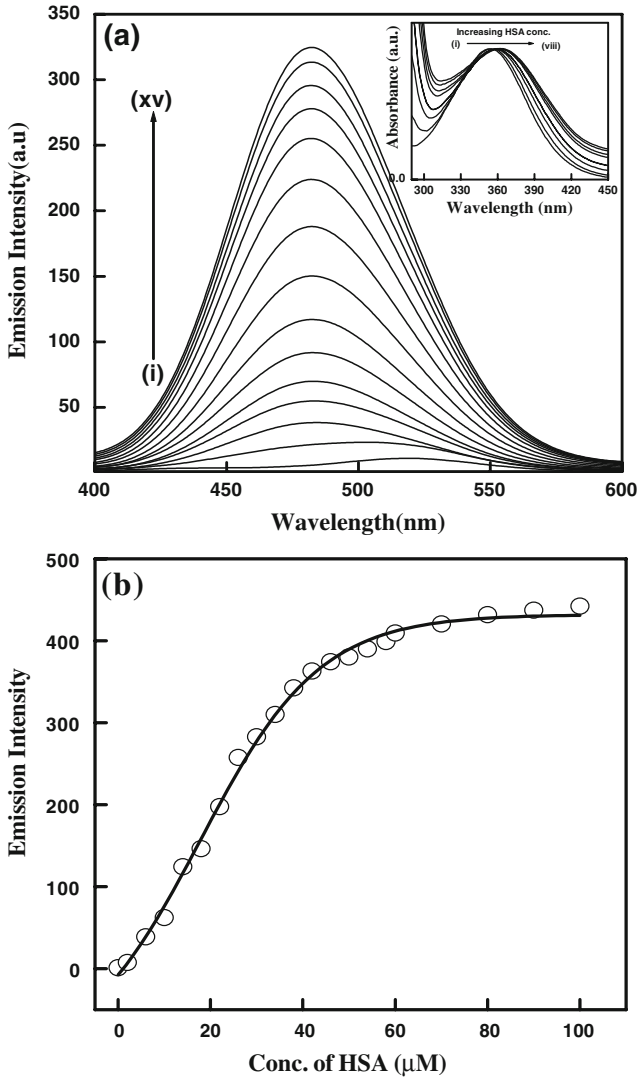

Fig. 1 (**a**) Effect of increasing concentration of HSA (0, 2, 6, 10, 18, 26, 34, 42, 46, 58, 60, 70, 80, 90 and 100 μM) on the fluorescence emission spectra (λ_{ext}=350 nm) of MDMANA (conc. of MDMANA 8.84 μM). (**b**) Plot of variation of the intensity of emission maxima of MDMANA with increasing concentration of HSA. *Inset*: (**a**) Effect of increasing concentration of HSA (0, 2, 6, 10, 14, 18, 22 and 30 μM on the absorption spectra of MDMANA (conc. of MDMANA 8.84 μM) (*arrow* indicates increasing HSA)

Where K is the binding constant for the complexation equilibrium. The concentration terms of each components of the above equation can be expressed in terms of fluorescence intensity. The main assumption is that the concentration of the complex is very low compared to that of the free protein. Therefore, the Benesi–Hildebrand relation for these types of complexation processes can be expressed in terms of intensity of emission as follows

$$I = \frac{I_0 + I_1 K[\mathrm{HSA}]}{1 + K[\mathrm{HSA}]} \tag{7}$$

Simplifying this we can have

$$\frac{1}{(I - I_0)} = \frac{1}{(I_1 - I_0)} + \frac{1}{(I_1 - I_0)K[\mathrm{HSA}]} \tag{8}$$

Where I_0, I and I_1 are the emission intensities in absence of, at intermediate and infinite concentration of HSA. As seen in Fig. 2, the plot of $1/[I–I_0]$ vs. 1/[HSA] gives a straight line indicating 1:1 complexation between MDMANA and HSA. The extent of binding, K is determined to be 1.14×10^4 M^{-1} from the ratio between intercept and slope of Benesi–Hildebrand plot (equation 8). The high value of K indicates strong binding between probe and protein molecules. Using the value of K, the free energy change, ΔG for such probe–protein complexation reaction is determined to be -23.16 kJ mol^{-1}. The values obtained for K and ΔG are well in agreement with that obtained for such complexation process studied earlier [13–17]. The negative free energy change indicates spontaneous complexation reaction between the fluorescence probe and protein HSA.

Steady state fluorescence anisotropy study

Complex biological membranes such as proteins form highly organized molecular assembly with considerable degree of anisotropy. As a result of this, the environment of the probe molecule inside such a complex molecular assembly solely depends on its precise location. Thus, the study of steady state fluorescence anisotropy is of immense importance and informative about the complex biological systems [27, 30]. The so-called environment-induced motional restriction on the mobility of the probe in a viscous or organized media can be assessed from the anisotropy values and hence the location of the probe

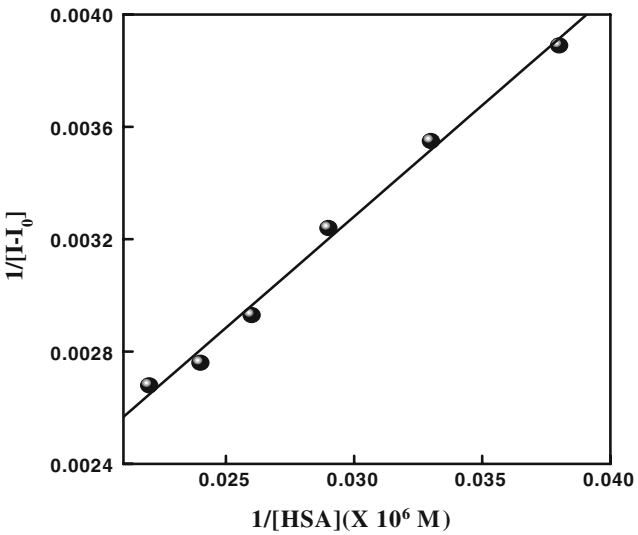

Fig. 2 Benesi–Hildebrand plot of $1/[I–I_o]$ vs. $1/[\mathrm{HSA}](M^{-1})$ for binding of MDMANA with HSA

molecule can be ascertained with high degree of efficiency. Figure 3 shows that the anisotropy values increase with increasing concentration of HSA. This indicates greater restriction experienced by the probe molecules upon binding with protein. It can however be seen in the figures that the anisotropy markedly increases up to 60 μM of HSA (0.406) and then become steady. Initial abrupt increase in anisotropy upon addition of protein is due to high rate of encapsulation of the probe molecules on coming in contact with the proteins and beyond 60 μM of HSA saturation of binding is reflected through unchanged values of anisotropy. The high anisotropy values indicate strong binding between MDMANA and HSA. It is complementary with the values of large complexation constant.

Polarity of the microenvironment around the fluorophore

Proteinous medium is a heterogeneous one and the probe molecules experience different polarity inside the protein than in the bulk. The CT band of MDMANA is found to be highly sensitive to polarity of a medium and hence the position of the CT band inside the proteinous environment could be a guiding factor to know about the micropolarity of the proteinous environment. It is seen that in protein solution (in Tris buffer) the CT band of MDMANA is blue shifted compared to the position of the CT band in water and hence we can say that the polarity of the proteinous environment is less than water. To find out the polarity experienced by our probe molecules inside the protein solution, we have taken MDMANA in different percentage of water and dioxane mixture and obtained $E_T(30)$ vs. λ^{max} plot (Fig. 4). From the graph the $E_T(30)$ value in HSA

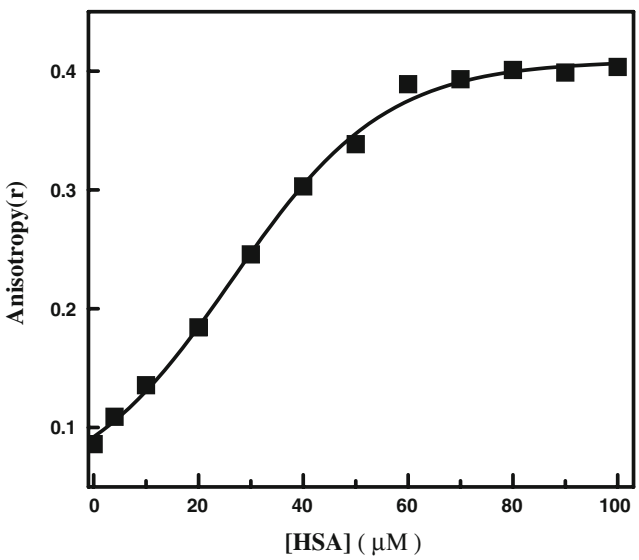

Fig. 3 Variation of steady state anisotropy (λ_{em}=482 nm and λ_{ext}= 350 nm) of MDMANA with increasing concentration of HSA

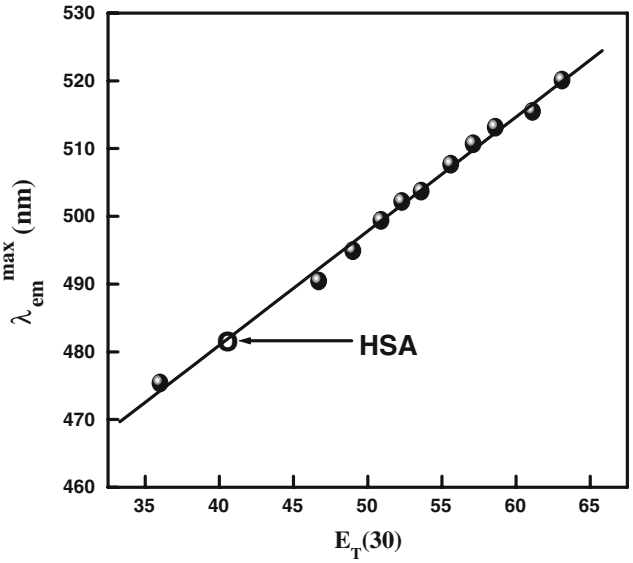

Fig. 4 Variation of emission maximum (λ_{em}^{max}) of MDMANA in the dioxane–water mixture against $E_T(30)$ parameters. The *open circles* give the interpolated λ_{em}^{max} values of HSA

medium is found to be 40.5. This value clearly indicates that the polarity of proteinous medium is slightly high compare to the polarity of pure dioxane but remarkably low compared to pure water [14, 17]. Due to less polar hydrophobic environment the emission of CT band is shifted to blue.

Wavelength-sensitive fluorescence parameters

Red Edge Excitation Shift (REES) [30–34] is a well known phenomenon which provides a more vivid picture of the surrounding atmosphere of the probe while emitting from the excited state. This technique comes in handy to monitor directly the environment and dynamics around a fluorophore in a complex biological system. An increase in REES values with increasing concentration of protein indicates greater restriction on the mobility of the solvent molecules surrounding the probe molecules bound within the hydrophobic cavity of the protein. As seen in Fig. 5, the molecule MDMANA exhibits a shift of the emission maxima towards the red end with shift in the excitation wavelength towards the red end. Solvatochromism measurement shows that the dipole moment of the CT state (12.22D) is quite high compared to that of the ground state (4.72D) [23]. As can be seen in Fig. 5, the REES value of ~4 nm for 30 μM HSA in medium is appreciable to predict a motionally restricted environment experienced by the probe molecule in proteinous media.

Fluorescence polarization is dependent on excitation wavelength in the restricted or organized media. Valeur and Weber interpreted this observation in terms of larger apparent molecular volume. Later on, Lakowicz explained

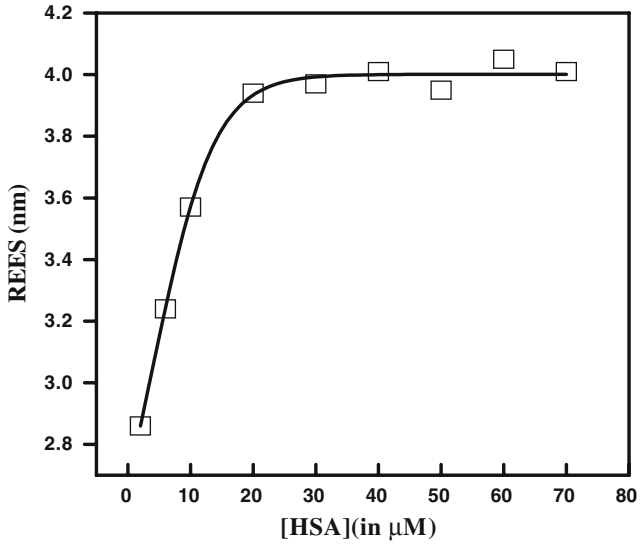

Fig. 5 Plot of REES values vs. concentration of HSA (μM)

this observation on the basis of decrease in rotational rate of the fluorophore in restricted media [32]. This was due to increased dipolar interaction of the fluorophore with the surrounding solvent dipoles. Increase in polarization value at a particular protein concentration with shifting of excitation wavelength to the red end, points towards the fact that the probe molecules lie in a motionally restricted environment [34]. A linear increase in polarization values with excitation wavelength is observed in case of MDMANA–HSA (Fig. 6). This arises due to slow rates of reorientation of the solvent molecules around the fluorophore in the excited state in organized media.

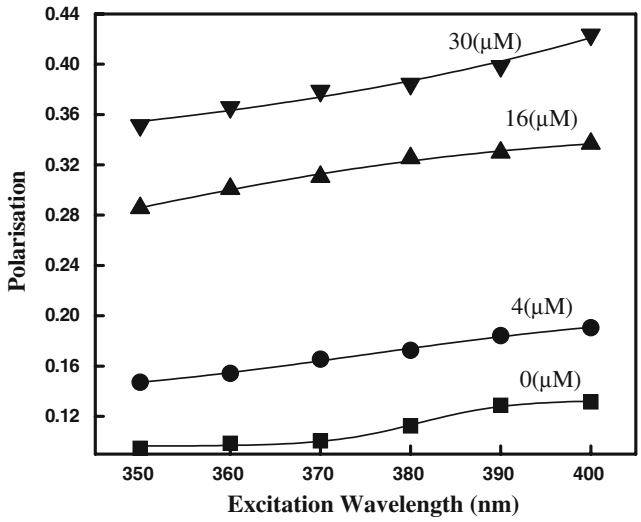

Fig. 6 Variation of steady state polarization values (λ_{em}=482 nm) of MDMANA with change in excitation wavelength at definite HSA concentrations in the medium

Steady state acrylamide quenching of MDMANA-HSA fluorescence

It is known that acrylamide shows an unusually high degree of static quenching of tryptophanyl fluorescence of Serum Albumins. Figure 7 shows that the addition of acrylamide to MDMANA–HSA complex in 20 μM of HSA results in a decrease in fluorescence intensity of the emission band at ~482 nm with slight red shift of the emission maxima (~482 nm to ~483 nm at 2M acrylamide in HSA). Acrylamide releases probe molecules from the hydrophobic sites by approaching close to the site. As the probe molecules are thrown out from hydrophobic site to the aqueous phase, the CT fluorescence gets quenched with red shift of the emission maxima [15]. The Stern–Volmer plot of I_0/I vs. [Acrylamide] gives a straight line (inset of Fig. 7). The Stern–Volmer quenching constant, K_{SV}= 0.94 M^{-1} is determined from the slope of the plot. The value of K_{SV} predicts the degree of exposure of the probe molecules to the aqueous phase. The value of K_{SV} obtained for quenching of MDMANA-HSA fluorescence indicates that the probe molecules lie deeply embedded in the hydrophobic pocket of the HSA molecules.

Fluorescence time-resolved measurements

The time-resolved studies of intrinsic fluorophore tryptophan are complex, because most proteins contain more than one tryptophan unit, which lies in different environment and secondly, protein folding and unfolding are very complex and fast processes and collection of suitable data ranges in hours. Under such circumstances, the fluores-

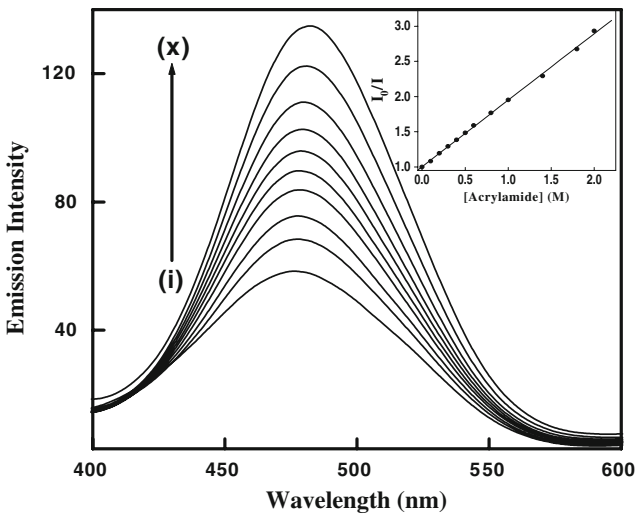

Fig. 7 (**a**) Variation of fluorescence emission spectra (λ_{ext}=350 nm) of MDMANA–HSA complex with increasing acrylamide concentration in 20 μM HSA; (*inset*) Stern–Volmer plot of I_0/I vs. [Acrylamide] in HSA

Table 1 Fluorescence lifetimes of MDMANA with increasing HSA concentration

Environment	a_1	a_2	a_3	τ_1	τ_2	τ_3	χ^2	$\langle\tau\rangle$ (ns)
HSA (4 μM)	0.376	0.539	0.085	0.451	0.111	1.487	1.40	0.931
HAS (100 μM)	0.4104	0.4078	0.1817	0.606	0.220	1.66	1.35	1.050

cence lifetimes of the probes bound to proteins throw light on the microenvironment surrounding the probe molecule and concrete inference can be drawn about the nature of protein-probe binding as well as conformational changes of proteins under various circumstances. The fluorescence decay curves for such binding processes in heterogeneous media are generally multiexponential. For MDMANA bound to HSA, the fluorescence decay curves were fitted best to triple exponential function with acceptable values for χ^2 (Table 1). As seen in Fig. 8, fluorescence lifetime of MDMANA increases with increasing HSA concentration. The origin of this triple exponential decay is not very clear. But, in analogy to other such studies, it can be said that different components may be due to binding of the probe to different binding sites of the protein. This increase in lifetime is due to decrease in non-radiative decay channels, which are operative in aqueous phase [13–17]. Due to encapsulation of the probe at the hydrophobic cavity, the exposure of the probe to water is less and hence non-radiative process is less. Though the lifetime of the probe in aqueous buffer could not be obtained due to its ultrafast nature, the lifetimes of the probe bound to proteins lied within the resolution limit (72ps) of the lifetime measuring instrument.

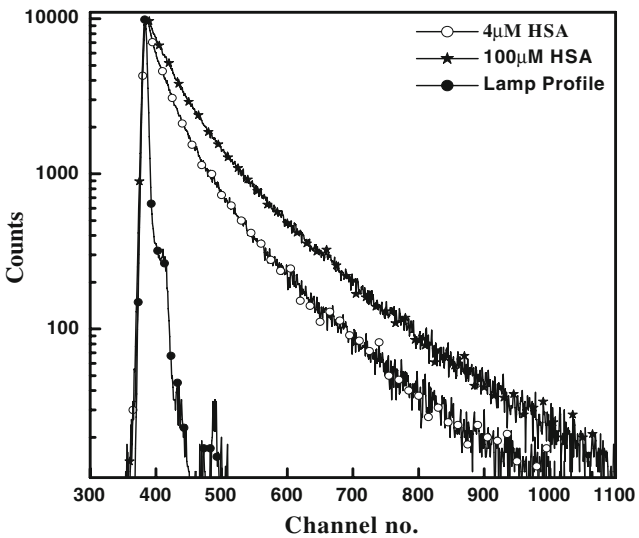

Fig. 8 Fluorescence decay curves of MDMANA with increasing HSA concentration

The quantum yield values (Table 2) indicate that the non-radiative pathways become less operative in the proteinous environment, however, they do not cease to exist completely as is evident from radiative (k_r) and non-radiative (k_{nr}) rate constants. The rate constants can be calculated using the following relations:

$$k_r = \Phi_f/\tau \tag{9}$$

$$1/\tau = k_r + k_{nr} \tag{10}$$

where Φ_f and τ are the fluorescence quantum yield and average fluorescence lifetime, respectively. The value of K_{nr} is indicative of the still present non-radiative channels though to a lesser extent than in pure aqueous medium. Stronger the binding, lesser is the probability of deactivation via non-radiative pathways and higher is the radiative lifetime of the probe molecule.

Fluorescence resonance energy transfer (FRET)

Fluorescence resonance energy transfer (FRET) [27–35] is a good technique to determine the distance (in nanometer scale) between donor fluorophore and acceptor fluorophore in vitro and in vivo. FRET is a distance dependent tool and is achieved by exciting the donor fluorophore at its specific excitation wavelength and this molecule by dipolar interaction transfers the energy non-radiatively to an acceptor molecule lying within Förster distance of 2–8 nm from it. The donor then returns to its electronic ground state. Though the energy transfer is via a non-radiative pathway, it is termed as 'Fluorescence Resonance Energy Transfer' (FRET) when both the donor and acceptor molecules are fluorescent. Basically the FRET efficiency depends on three parameters—(i) the distance between donor and acceptor must be within the specified Förster distance of 2–8 nm; (ii) there must be appreciable overlap between donor fluores-

Table 2 Quantum yields and rate constant for radiative and non-radiative decay in different microenvironments

Environment	Quantum Yield* Φ_f	k_r (s^{-1})	k_{nr} (s^{-1})
Aqueous buffer	0.003	–	–
HAS (100 μM)	0.093	0.088×10^9	0.864×10^9

cence and acceptor absorption band and (iii) proper orientation of the transition dipole of the donor and the acceptor fluorophore. During FRET process the emission intensity of the donor fluorophore decreases and acceptor fluorophore increases with a definite isoemissive point. According to Förster, the efficiency (E) of FRET process depends on the inverse sixth-distance between donor and acceptor (r) as well as critical energy transfer distance or Förster radius (R_0) under the condition of 1:1 situation of donor: acceptor concentrations and can be expressed by following equation

$$E = \frac{R_0^6}{R_0^6 + r^6} = 1 - \frac{I}{I_0} \tag{11}$$

where E is the efficiency of energy transfer; I and I_0 are the fluorescence intensities of donor in presence and absence of the acceptor respectively. R_0 is expressed as

$$R_0^6 = 8.8 \times 10^{-25} k^2 n^{-4} \phi_D J \tag{12}$$

where k^2 is the spatial orientation factor; n is the refractive index of the medium, ϕ_D is the fluorescence quantum yield of the donor and J is the overlap integral of emission spectrum of donor and acceptor spectrum of acceptor (Fig. 9a). The term J is expressed as

$$J = \frac{\int_0^\infty I(\lambda)\varepsilon(\lambda)\lambda^4 d\lambda}{\int_0^\infty I(\lambda) d\lambda} \tag{13}$$

where $I(\lambda)$ is the normalized fluorescence intensity in the range λ and $\lambda+\Delta\lambda$; $\varepsilon(\lambda)$ is the extinction coefficient of acceptor at λ. The overlap integral J is obtained by integrating the spectra in Fig. 9a. As shown in Fig. 9a, there is a good overlap between the emission spectrum of tryptophan with the absorption spectra of the probe MDMANA. Using the values of k^2=2/3, n=1.333 and ϕ_D=0.14 the data obtained are as follows: J=3.298×10^{-13} cm^2, R_0=4.52 nm and r=3.96 nm. The value of r indicates that the donor and acceptor are very closer to each other and hence have stronger binding between them.

Figure 9b shows the intrinsic fluorescence spectra of Trp-214 of HSA with increasing concentration of acceptor MDMANA. As seen in the figure, with increase of MDMANA concentration, the emission intensity of tryptophan decreases with the emergence of a new band at ~490 nm. This new band arises from the CT emission of MDMANA molecule bound to HSA which fluoresces after absorption of the photon emitted by the tryptophan of HSA. The efficiency of energy transfer is calculated using equation. It is found that the energy transfer efficiency from tryptophan to charge transfer probe is about 69.8%. As the probe is very closer to the protein, efficiency of energy transfer is very high.

Study of refolding of urea denatured protein by SDS

It is known that the denaturation of protein by urea can be protected to some extent by anionic surfactant SDS. In fact, during unfolding of protein HSA with urea the bound fluorophore MDMANA try to expose more to free solvents. As a result the polarity sensitive CT band should be affected. From Fig. 10a it is seen that the CT emission of MDMANA is red shifted with increasing urea concentration. The position of the CT emission band of MDMANA shifts slowly up to 6M urea concentration and there is a sharp rise of up to 10M urea concentration (Fig. 10b). This indicates that the micropolarity of the protein environment

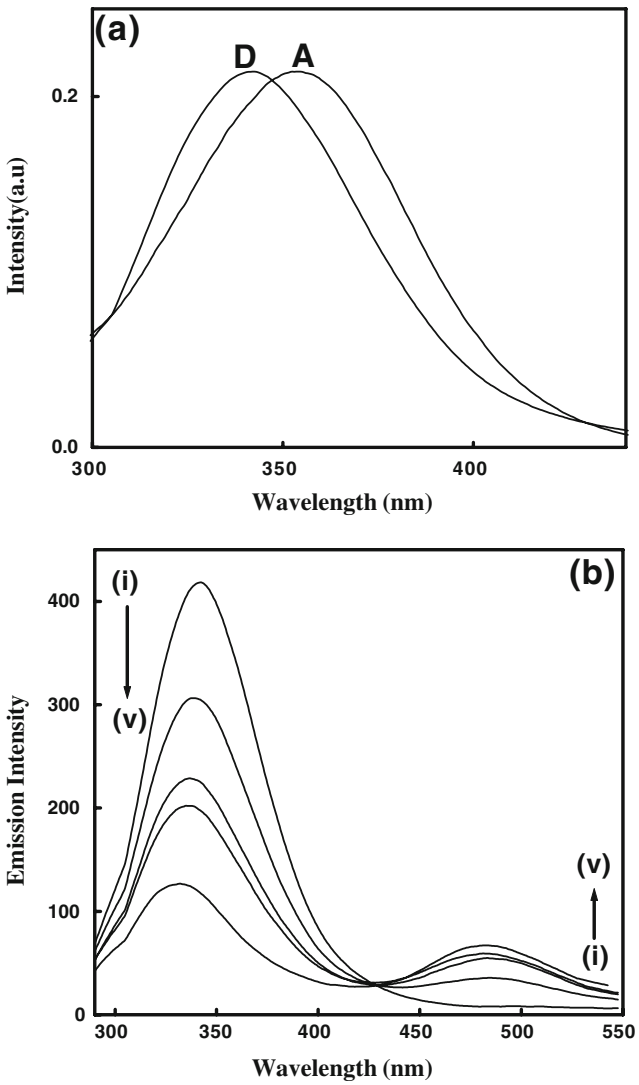

Fig. 9 (**a**) Fluorescence spectrum (λ_{ext}=290 nm) of tryptophan of HSA (20 μM) and absorption spectrum of probe MDMANA, (**b**) fluorescence spectra of tryptophan of HSA with increasing concentration of MDMANA (0, 8.84, 17.68, 35.36 and 44.2 μM)

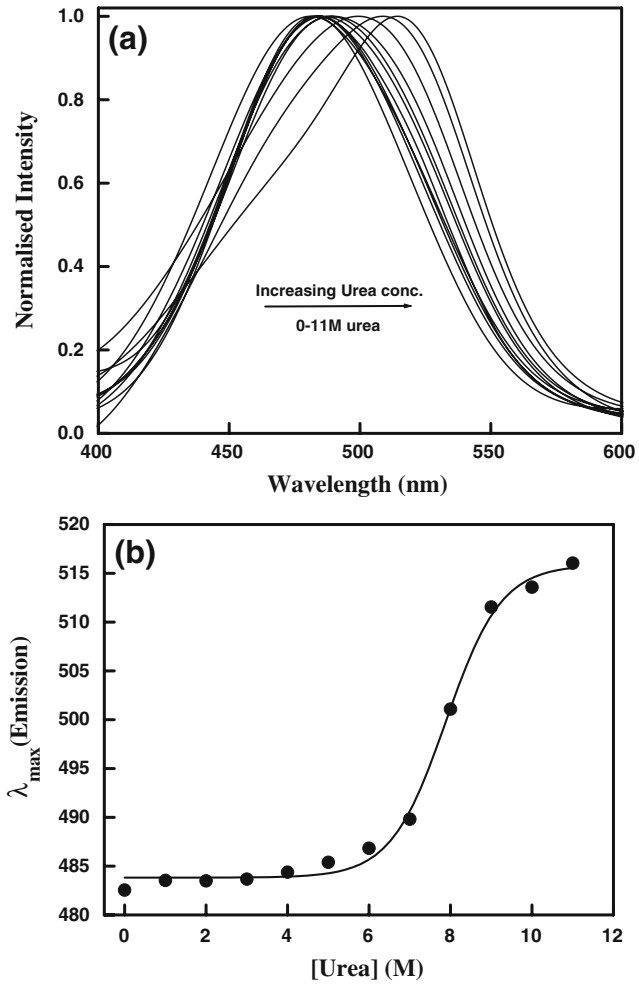

Fig. 10 (**a**) Normalized fluorescence emission spectra of MDMANA–HSA complex with increasing concentration of urea (0–11M); (**b**) plot of emission maxima (λ_{max}) of MDMANA–HSA complex at different concentrations of urea (0–11 M)

at different urea concentration is different and the CT probe clearly reflects the nature of microenvironment by its emission characteristics.

Urea is a stronger denaturant of HSA compared to SDS and the denaturing action of urea is merely based on breaking of water structures that stabilize the native conformation of proteins [12]. On the other hand surfactant SDS binds to the hydrophobic sites of the protein molecule resulting in uncoiling of the protein structure. The surfactant SDS, however, plays a dual role—as a stabilizer for urea-denatured HSA and a destabilizer for native conformation. MDMANA being hydrophobic in nature remains solubilized within hydrophobic cavity of HSA. Addition of urea results in denaturation of HSA and the probe molecules become exposed to the aqueous phase as mentioned earlier. Hence the polarity sensitive CT band shows a red shift. As seen in Fig. 11a & b, the protective action of SDS on the native structure of urea denatured HSA is well reflected through the shifting of the CT band along with denaturation and renaturation of HSA. The urea concentrations are roughly divided into three ranges [12].

i) Below 3M urea, the addition of SDS results in further denaturation of HSA and hence the CT band shows a red shift up to 2mM SDS and finally attains constancy (Fig. 12).
ii) The range between 4 M to 8 M urea where addition of SDS results in initial restoration of HSA conformation up to 0.15 mM SDS then further addition of SDS results in denaturation of HSA. This phenomenon is well reflected in terms of spectral shift of CT band of MDMANA. Initial recoiling of HSA on addition of SDS results in a blue shift of CT band and further

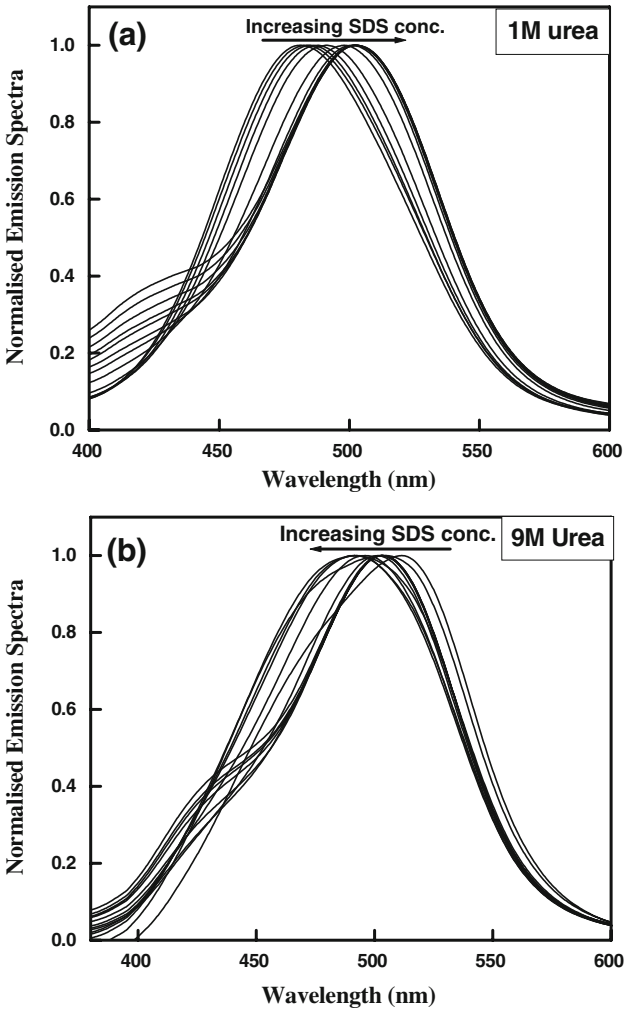

Fig. 11 Normalized emission spectra of MDMANA in urea denatured HSA medium with increasing SDS concentration in (**a**) 1 M and (**b**) 9 M urea

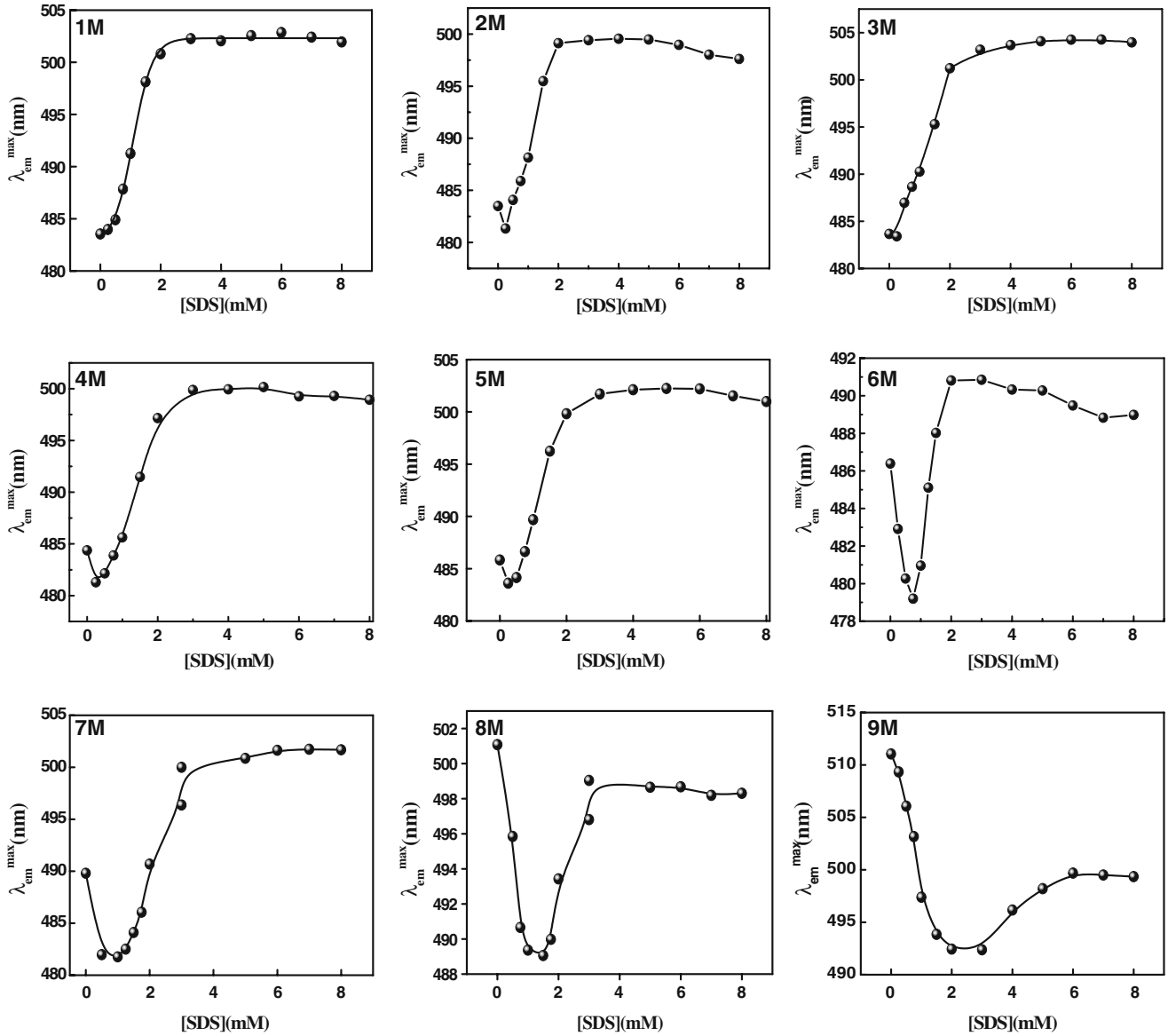

Fig. 12 Plots of emission maxima (λ_{em}^{max}(nm)) vs SDS concentration to show the helicity changes of HSA upon the addition of SDS to the protein denatured in the urea solution of various concentrations

addition results in a red shift of the CT band indicating greater exposure of probe molecules to aqueous phase (Fig. 12).

iii) At above 8M urea concentration addition of SDS results in only increase in helicity of HSA is reflected by blue shift of the CT band of MDMANA in urea-denatured HSA (Fig. 12). Here there is a minima at above 2 mM of SDS and then decrease in helicity occurs with increase of SDS concentration.

Thus, TICT probe MDMANA is successfully utilized in probing the conformational changes of urea-denatured HSA induced upon SDS binding.

Conclusion

In this paper the binding phenomenon of charge transfer probe MDMANA with human serum albumin (HSA) is explored using absorption and fluorescence spectroscopic methods. The results indicate that MDMANA can be successfully used for studying the polarities of protein cavities. Red shift of the absorption maxima and blue shift of emission maxima with manifold enhancement of intensity on addition of HSA indicates complexation of MDMANA with HSA. High value of binding constant, $K = 1.14 \times 10^4 M^{-1}$ and free energy change $\Delta G = -23.16$ kJ/mol indicates strong binding between probe and protein and spontaneous complexation process. Increasing values of

steady state fluorescence anisotropy and REES of MDMANA with increasing of HSA concentration as well as increasing polarization values with excitation wavelength point towards the fact that probe molecules get trapped within the hydrophobic pockets of HSA indicating lesser freedom on mobility of probe inside the protein cavity. Fluorescence lifetime measurement and FRET study also supports strong binding of the probe with the protein with efficient energy transfer process. Protective action of SDS to urea-denatured HSA in different urea concentration can be easily demonstrated using MDMANA as fluorescence probe. Thus, the sensitivity of charge transfer probe MDMANA to slight changes in the micropolarity of its surrounding environment makes it an efficient fluorescent probe for studies in proteinous environments.

Acknowledgement NG gratefully acknowledges the financial support received from Department of Science and Technology, India (Project No.SR/S1/PC-1/2003). RBS and SM thank CSIR, New Delhi for research fellowship. The authors are thankful to Dr. Nilmoni Sarkar and Mr. Debabrata Seth of Department of Chemistry, IITKGP for fluorescence lifetime measurements.

References

1. Peters T Jr (1985) Serum albumin. Adv Protein Chem 37:161 doi:10.1016/S0065-3233(08)60065-0
2. Carter DC, Ho JX (1994) Structure of serum albumin. Adv Protein Chem 45:153 doi:10.1016/S0065-3233(08)60640-3
3. Brown JR (1977) Albumin structure, function and uses. Pergamon, Oxford, p 27
4. Carter DC, He XM, Munson SH, Twigg PD, Gernert KM, Broom MB et al (1989) Three-dimensional structure of human serum albumin. Science 244:1195 doi:10.1126/science.2727704
5. He XM, Carter DC (1992) Atomic structure and chemistry of human serum albumin. Nature 358:209 doi:10.1038/358209a0
6. Sudlow G, Birkett DJ, Wade DN (1977) Further characterization of specific drug binding sites on human serum albumin. Mol Pharmacol 12:1052
7. Moreno F, Cortijo M, Gonzalez-Jimenez J (1999) The fluorescent probe prodan characterizes the warfarin binding site on human serum albumin. Photochem Photobiol 69:8
8. Kumar CV, Buranaprapuk A (1999) Tuning the selectivity of protein photocleavage: spectroscopic and photochemical studies. J Am Chem Soc 121:4262 doi:10.1021/ja9844377
9. Reed RG (1977) Nucleus-dependent regulation of tyrosine aminotransferase degradation in hepatoma tissue culture cells. J Biol Chem 252:7483
10. Jacobsen J, Brodersen R (1983) Location of long chain fatty acid-binding sites of bovine serum albumin by affinity labeling. J Biol Chem 258:6319
11. Markus G, Karush F (1957) Structural effects of the interaction of human serum albumin with sodium decyl sulfate. J Am Chem Soc 79:3264 doi:10.1021/ja01569a073
12. Moryama Y, Sato Y, Takeda K (1993) Reformation of helical structure of bovine serum albumin by the small amount of sodium dodecyl sulphate after the disruption of the structure by urea. J Colloid Interface Sci 156:420 doi:10.1006/jcis.1993.1132
13. Banerjee A, Basu K, Sengupta PK (2008) Interaction of 7-hydroxyflavone with human serum albumin: a spectroscopic study. J Photochem Photobiol B Chem 90:33
14. Mallick A, Haldar B, Chattopadhyay N (2005) Spectroscopic investigation on the interaction of ICT probe 3-Acetyl-4-oxo-6,7-dihydro-12H Indolo-[2,3-a] quinolizine with serum albumins. J Phys Chem B 109:14683 doi:10.1021/jp051367z
15. Davis DM, Birch DJS (1996) Extrinsic fluorescence probe study of human serum albumin using nile red. J Fluoresc 6:23 doi:10.1007/BF00726723
16. Wu F-Y, Ji Z-J, Wu Y-M, Wan X-F (2006) Interaction of ICT receptor with serum albumins in aqueous buffer. Chem Phys Lett 424:387 doi:10.1016/j.cplett.2006.05.019
17. Singh RB, Mahanta S, Guchhait N (2008) Study of interaction of proton transfer probe 1-hydroxy 2-naphthaldehyde with serum albumins: spectroscopic study. J Photochem Photobiol B Biol 91:1 doi:10.1016/j.jphotobiol.2007.12.006
18. Kaldas MI, Walle UK, van der Woude H, McMillan JM, Walle T (2005) Covalent binding of the flavonoid quercetin to human serum albumin. J Agric Food Chem 53:4194 doi:10.1021/jf050061m
19. Papadopoulou A, Green RJ, Frazier RA (2005) Interaction of flavonoids with bovine serum albumin: a fluorescence quenching study. J Agric Food Chem 53:158 doi:10.1021/jf048693g
20. Sahu K, Mondal SK, Ghosh S, Roy D, Bhattacharyya K (2006) Temperature dependence of solvation dynamics and anisotropy decay in a protein: ANS in bovine serum albumin. J Chem Phys 124:124909 doi:10.1063/1.2178782
21. Buzady A, Savolainen J, Erostyak J, Myllyperkio J, Somogyi B, Korppi-Tommola J (2003) Femtosecond transient absorption study of the dynamics of acrylodan in solution and attached to human serum albumin. J Phys Chem B 107:1208 doi:10.1021/jp027107o
22. Amisha Kamal JK, Zhao L, Zewail AH (2004) Ultrafast hydration dynamics in protein unfolding: human serum albumin. Proc Natl Acad Sci U S A 101:13411 doi:10.1073/pnas.0405724101
23. Mahanta S, Singh RB, Kar S, Guchhait N (2008) Photoinduced intramolecular charge transfer in methyl ester of N, N'-Dimethyl aminonaphthyl-(acrylic)-acid: Spectroscopic measurement and quantum chemical calculations. J Photochem Photobiol Chem A 194:318
24. Turro NJ, Lei X-G (1995) Spectroscopic probe analysis of protein–surfactant interactions: the BSA/SDS system. Langmuir 11:2525 doi:10.1021/la00007a035
25. Das R, Guha D, Mitra S, Kar S, Lahiri S, Mukherjee S (1997) Intramolecular charge transfer as probing reaction: fluorescence monitoring of protein–surfactant interaction. J Phys Chem A 101:4042 doi:10.1021/jp9625669
26. Mahanta S, Singh RB, Kar S, Guchhait N (2007) Excited state intramolecular proton transfer in 3-hydroxy-2-naphthaldehyde: a combined study by absorption and emission spectroscopy and quantum chemical calculation. Chem Phys 324:742 doi:10.1016/j.chemphys.2006.01.036
27. Lakowicz JR (1999) Principles of fluorescence spectroscopy. Plenum, New York
28. Chakraborty A, Seth D, Setua P, Sarkar N (2006) Photoinduced electron transfer in a protein-surfactant complex: probing the interaction of SDS with BSA. J Phys Chem B 110:16607 doi:10.1021/jp0615860
29. Benesi HA, Hildebrand JH (1949) A spectrophotometric investigation of the interaction of iodine with aromatic hydrocarbons. J Am Chem Soc 71:2703 doi:10.1021/ja01176a030
30. Valeur B, Weber G (1977) Anisotropic rotations in 1-naphthylamine. Existence of Red-edge transition moment normal to the ring plane. Chem Phys Lett 45:140 doi:10.1016/0009-2614(77)85229-9

31. Weber G, Schinitzky M (1970) Failure of energy transfer between identical aromatic molecules on excitation at the long wave edge of the absorption spectrum. Proc Natl Acad Sci U S A 65:823 doi:10.1073/pnas.65.4.823
32. Lakowicz JR, Nakamoto SK (1984) Red-edge excitation of fluorescence and dynamic properties of proteins and membranes. Biochemistry 23:3013 doi:10.1021/bi00308a026
33. Itoh K, Azumi T (1975) Shift of the emission band upon excitation at the long wavelength absorption edge. II. Importance of the solute–solvent interaction and the solvent reorientation relaxation process. J Chem Phys 62:3431 doi:10.1063/1.430977
34. Mukherjee S, Chattopadhyay A (1995) Wavelength-selective fluorescence as a novel tool to study organization and dynamics in complex biological systems. J Fluorescence 3:237 doi:10.1007/BF00723895
35. Struck DK, Hoekstra D, Pagano RE (1981) Use of resonance energy transfer to monitor membrane fusion. Biochemistry 20:4093 doi:10.1021/bi00517a023